Monolayer characteristics and spectroscopic study of benz(b)fluoranthene assembled in Langmuir Blodgett films mixed with stearic acid

ARTICLE *in* JOURNAL OF PHYSICS AND CHEMISTRY OF SOLIDS · JUNE 2003

Impact Factor: 1.85 · DOI: 10.1016/S0022-3697(02)00367-0

3 AUTHORS, INCLUDING:

Somobrata Acharya

Indian Association for the Cultivation of Scie…

81 PUBLICATIONS **2,055** CITATIONS

SEE PROFILE

ELSEVIER

Journal of Physics and Chemistry of Solids 64 (2003) 651–657

JOURNAL OF PHYSICS AND CHEMISTRY OF SOLIDS

www.elsevier.com/locate/jpcs

Monolayer characteristics and spectroscopic study of benz(*b*)fluoranthene assembled in Langmuir Blodgett films mixed with stearic acid

S. Acharya[a], D. Bhattacharjee[b], G.B. Talapatra[a,*]

[a]*Department of Spectroscopy, Indian Association for the Cultivation of Science, Jadavpur, Calcutta 700 032, India*
[b]*Department of Physics, Tripura University, Suryamaninagar, Tripura 799130, India*

Received 13 December 2001; accepted 23 July 2002

Abstract

Excellent Langmuir Blodgett (LB) films of benz(*b*)fluoranthene (B(*b*)F) have been prepared by mixing with stearic acid (SA). The surface pressure vs. area per molecule isotherms (π–A) of B(*b*)F mixed with SA at different mole fraction reveal that the area per molecule decreases with increasing mole fractions of B(*b*)F. The area per molecule vs. mole fraction shows that there is positive deviation of the experimental data to the idealized one. This indicates formation of aggregation of B(*b*)F molecules in the SA matrix. Spectroscopic properties of B(*b*)F in solution and in mixed LB films have been compared by absorption, steady state fluorescence, phosphorescence spectroscopy and lifetime measurements. Bathochromic shift in absorption and emission spectrum suggests the formation of some kind of aggregates in LB film. Decrease in fluorescence and phosphorescence lifetime is compared to that of pure B(*b*)F also supports the formation of different sized aggregates in the mixed film.

1. Introduction

Langmuir Blodgett (LB) films are constructed by transferring monolayers floating on an interface (generally air–water) to a solid substrate. Thickness and molecular arrangement of such films are controllable at the molecular level. Due to restricted motion of chromophores, highly precise orientation, etc. the photophysical processes of electronically excited molecules in LB films are generally quite different from those of solution or bulk. Nonamphiphilic molecules are not ideally suited to thin film deposition by this technique. However, studies [1–17] suggest that mixing with a long chain fatty acid or an inert polymer matrix can form high quality LB films of these materials. The spectroscopic properties of such films are quite similar to the amphiphilic counterparts. Investigations on LB films have emerged in the forefront of research as they are expected to be widely applicable to molecular electronic and bio-electronic devices [10,18]. Although, these studies have received considerable attention, still the role of π-electron conjugation, ultra structure as well as domain structure on electrical, optical and spectroscopic properties is not very clearly understood. Thus, a thorough understanding of the basic physics involved in those properties of such films is a topic of fundamental importance.

The nonamphiphilic polycyclic aromatic hydrocarbons (PAH) are one of the most important and ubiquitous environmental pollutants. They are relevant for human health, because during breathing, the PAH-contaminated particles are transported into the human lung and are deposited there [19]. Therefore, it is relevant to study PAH based LB films which closely mimic biological membranes.

Here in this paper, we have studied the monolayer characteristics of B(*b*)F mixed with SA at the air–water interface in order to understand the compatibility of the host and guest. Properties of mixed LB film have been discussed in the light of UV–Vis absorption, emission, fluorescence

* Corresponding author. Fax: +91-3-34732805.
E-mail address: spgbt@mahendra.iacs.res.in (G.B. Talapatra).

0022-3697/03/$ - see front matter © 2003 Elsevier Science Ltd. All rights reserved.
PII: S0022-3697(02)00367-0

lifetime measurement, and phosphorescence spectra in detail. These studies suggest the formation of some kind of aggregate in mixed LB film.

2. Experimental

B(*b*)F was a product of Aldrich Chemical Co., USA, and was vacuum sublimed followed by repeated recrystallization before use. SA (purity > 99%) from Sigma, USA was used as received. The solvents, ethanol (E. Mark, Germany) and chloroform (SRL, India) are of spectral grade and their fluorescence spectra were checked before use. A commercially available alternate layer LB trough (Joyce-Loebl, model 4 manufactured by Joyce-Loebl Inc. UK) was used for isotherm measurement and for multilayer film deposition. The subphase used was triple-distilled water further deionized with a Milli-Q plus water purification system from Millipore, USA. The pH of the subphase was 6.5 in equilibrium with atmospheric carbon dioxide, its resistivity was 18.2 MΩ cm and the temperature was 23 °C, respectively. Solution of B(*b*)F, SA as well as also B(*b*)F–SA mixture in different mole fractions were prepared in chloroform and were spread on the subphase. After a delay of 15 min to allow the solvent to evaporate, the film was slowly compressed for the measurement of the isotherms at room temperature (23 °C). The barrier compression rate was 2×10^{-3} nm^2 molecule^{-1} s^{-1}. Pressure increase was recorded using Wilhelmy plate arrangement as described elsewhere [12]. All isotherms were run at least three times with freshly prepared mixtures of B(*b*)F–SA at predetermined ratio. The accuracy of the system under the conditions in which the measurements were performed was 0.5 mN/m for surface pressure. Deposition of multilayers was achieved by allowing the substrate to dip with a speed of 5 mm min^{-1} with a drying time of 30 min after each lift. Fluorescent-grade quartz slides were used for spectroscopic measurements. The transfer ratio was calculated from the ratio of the total decrease of the surface of the film at the air–water interface and the total surface area of the substrate covered by the film multiplied by the number of layers deposited on the substrate. The transfer ratio was found to be 0.93 ± 0.02 on quartz slides.

Absorption spectra were recorded with a Shimadzu UVPC 2101 UV–Vis spectrophotometer. The polarized absorption spectra were recorded using UV–Vis polarizer accessories including a UV linear dichroic polarizer purchased from Oriel instruments, USA. For recording the emission spectra, a Hitachi, model F-4500 fluorescence spectrophotometer was used. The fluorescence lifetimes were measured by TCSPC technique (fluorometer, Applied Physics) using nitrogen filled nanosecond flash lamp. The apparatus was described earlier [20,21]. The full width at half maximum (FWHM) of the pump function was of the order of 1.9 ± 0.1 ns. The fluorescence decay curve analysis was performed by a deconvolution technique, where the experimental data are compared with a model decay function. The decay parameters were determined by a least squares fitting routine; the goodness of the fit was assessed by the reduced χ^2 values (good results typically produce values in the range 0.9–1.2), as well as by the randomness of the weighted residuals. All measurements were carried out at 298 K. The temperature was controlled by a Neslab thermostat using water as heat carrier. For the preparation of ethanol glass matrix, the solution of B(*b*)F in ethanol was kept in a quartz tube. The tube was then inserted within a dewer containing liquid nitrogen (77 K). The liquid column with in the quartz tube is solidified and appears to be a transparent glass.

The F-4500 Hitachi phosphorescence accessory was used to measure phosphorescence spectra and lifetimes. All phosphorescence measurements were performed at 77 K.

3. Results and discussion

3.1. Behavior of Langmuir monolayers

In Fig. 1, we have plotted the surface pressure (π) vs. area per molecule (*A*) isotherms of pure SA, pure B(*b*)F and B(*b*)F–SA mixed film at different mole fractions of B(*b*)F. When a solution of pure B(*b*)F in chloroform (1×10^{-3} M) was spread at the air–water interface and the barrier was compressed slowly, it was observed that it does not give rise to a compact monolayer but instead formed microcrystals (MCs) which were pushed together in the compression process and the surface pressure hardly rises to 18 mN/m. On relaxing the surface pressure, the MCs broke up into smaller sizes but did not disintegrate completely. Identical results have been reported for other nonamphiphilic PAH namely pyrene [12], chrysene [22], *p*-terphenylene [23]. Repeated attempts to transfer the floating layer of pure B(*b*)F onto quart slides failed. While attempting to transfer the floating layer of pure B(*b*)F onto quartz slide, an inhomogenous patchy film was observed. However, mixing B(*b*)F with SA, stable floating monolayer was obtained which could be transferred onto solid substrates with good transfer ratios (0.93 ± 0.02).

The area per molecule for pure SA extrapolated at the surface pressure of 25 mN/m is 0.22 nm^2 and is in good agreement with the data reported elsewhere. Also the area per molecule for pure B(*b*)F extrapolated at the surface pressure of 15 mN/m is 0.04 nm^2 as shown in Fig. 1. The area per molecule for pure B(*b*)F is found to be considerably less than the actual planar area of the molecule as predicted by the space-filling model. This indicates that the B(*b*)F molecules do not lie flat at the air–water interface but form multilayers or aggregates of pure B(*b*)F molecules. By the way, Benz(k)fluoranthene which is another member of the PAH family and having same planer area and molecular weight [19] as that of B(*b*)F, shows similar result [9].

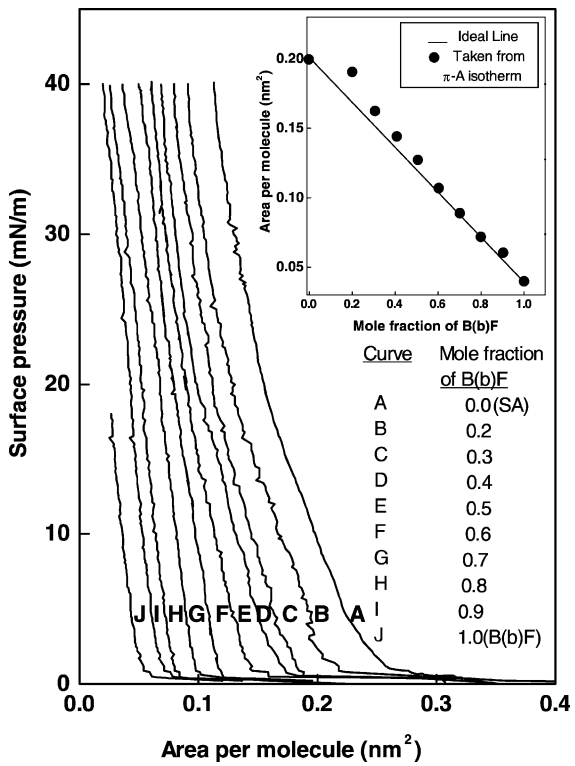

Fig. 1. Surface pressure vs. area per molecule at different mole fraction of B(b)F and SA. The inset shows plot of area per molecule vs. mole fraction of B(b)F molecules.

However, when B(b)F is mixed with SA, it forms quite stable compressible monolayer and surface pressure rises to about 40 mN/m. With the increase of mole fraction of B(b)F, we observe a decrease in area per molecule of the mixed system. The decreases in area per molecule as observed in the isotherm curve may be due to immersion of organic B(b)F in water. This possibility was ruled out as we do not observe any emission from the aliquot collected from the deep inside of the subphase below the layer as was stated in earlier paper [6]. So the decrease is due to the accommodation of B(b)F molecules within the SA matrix. In the monolayer there are three types of interactions; SA–SA, SA–B(b)F and B(b)F–B(b)F. Among these three interactions, SA–B(b)F interaction helps in the formation and stability of monolayer. However, if B(b)F–B(b)F interaction predominates over SA–B(b)F interaction, then B(b)F molecules tend to assimilate and may form 2D or 3D aggregates and the area per molecule is expected to decrease.

The π–A isotherms at the air–water interface provide information not only about the orientation of the molecule but also on the interactions between the constituent molecules of the mixed monolayers. From the isotherms of B(b)F–SA mixed systems, the average area per molecule at 5 mN/m surface pressure was obtained and plotted in the inset of Fig. 1 for various B(b)F mole fractions. For a two component system of noninteracting molecules the average area is given by the additivity rule [24–26]

$$A_{\mathrm{B}(b)\mathrm{F-SA}} = N_{\mathrm{B}(b)\mathrm{F}} A_{\mathrm{B}(b)\mathrm{F}} + N_{\mathrm{SA}} A_{\mathrm{SA}}$$

where $A_{\mathrm{B}(b)\mathrm{F-SA}}$ is the average area per molecule for the mixed monolayer of B(b)F and SA. $N_{\mathrm{B}(b)\mathrm{F}}$, N_{SA}, $A_{\mathrm{B}(b)\mathrm{F}}$ and A_{SA} correspond to the mole fraction and the area per molecule of pure B(b)F and SA, respectively.

Interestingly, the experimental data points show positive deviation from the ideal curve. This indicates a repulsive interaction between the components that may result in aggregation of B(b)F molecules in the mixed films. This is consistent with the behavior of other nonamphiphilies [13,27].

4. Electronic spectra

4.1. Absorption spectroscopic study

Fig. 2 shows the absorption spectra of the mixed LB films at various mole fractions of B(b)F (0.1–0.6 M B(b)F) in SA matrix, along with the spectra in ethanol solution, ethanol–water mixture and MC for comparison. The absorption spectrum of B(b)F in ethanol solution (1×10^{-6} M) consists of distinct and intense band systems in the 200–400 nm spectral region with the 0–0 band at about 368 nm. The intense set of bands in the region 230–310 and 310–370 nm in solution spectra corresponds to well defined ^1B_b and ^1L_a states of fluoranthene molecule according to Plat's classification (β and p bands in Clar's notation) [28,29]. The LB films absorption spectra at different mole fractions of B(b)F in SA matrix shows that all the band systems are broadened. However, no significant changes in the spectra were obtained by changing the mole fraction of B(b)F in LB films. The 0–0 band of the B(b)F LB film is red shifted to about 378 nm. Such bathochromic shift may arise from differences in the refractive indices and dielectric constants in different solvents. However, in less polar SA such shift is unlikely. The shift and broadening observed in the mixed LB films may be related to a well-defined molecular arrangement using a dipole model. According to exciton model of McRay and Kasha [30,31], the exciton band formed as a result of dipole–dipole interaction. The energetic position of such a band with respect to the monomeric band depends on the angle, θ, made by the dipole moment with the vector r, joining the centers of the two dipoles. The change in energy due to such an interaction is mathematically expressed as $\Delta E = 2\mu^2(1 - 3\cos^2\theta)/r^3$, where μ is the dipole moment. When the alignment of the dipole moments in the aggregates is such that $0 < \theta < 54.7°$, the exciton band is located energetically below the monomeric state, which gives a red shifted absorption spectrum and the aggregates are referred to as J-type aggregates [32]. In this context, it is

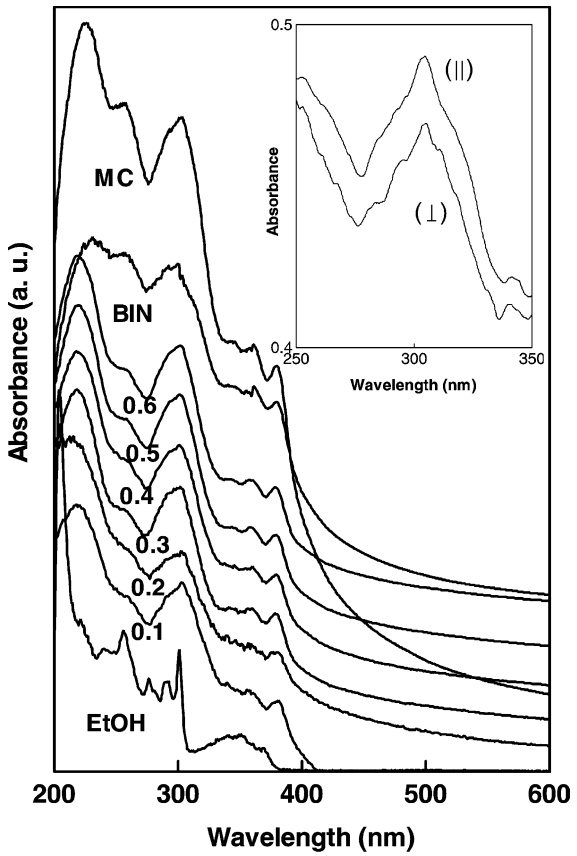

Fig. 2. Electronic absorption spectra of B(*b*)F in ethanol solution (EtOH), MC and BIN as well as in mixed LB films with SA at different B(*b*)F mole fractions. The inset shows polarized absorption spectra of mixed B(*b*)F–SA LB film (0.5 mole fraction of B(*b*)F) for polarization parallel (||) and perpendicular (⊥) to the dipping direction.

relevant to mention that the effect of aggregation on optical absorption spectrum may also be accounted precisely by applying extended dipole approximation model of Kuhn [33]. This model gives better agreement with the experimentally observed shift in absorption spectra due to formation of aggregate. However, the absence of intense narrow absorption and an almost coinciding fluorescence peak (characteristics of J-band) makes the structural assignment difficult.

To confirm the formation of aggregates, we have considered another established method of producing aggregates [34]. We have used ethanol–water mixture as solvent. The presence of water in the mixture promotes hydrophobic interaction, which results in the molecular association of the aromatics. The absorption spectra of mixed LB films of B(*b*)F show similar type of shifting and broadening (Fig. 2) as in ethanol–water mixture (volume fraction of water 0.4) and B(*b*)F MC spectra suggesting formation of aggregates in the LB films.

Polarized absorption spectrum has often been used to study the orientation of the chromophores in the mixed LB films [13]. The inset of Fig. 2 shows the polarized absorption spectra of B(*b*)F and SA LB film (0.5 mole fraction of B(*b*)F; $\pi = 25$ mN/m) at an angle of incidence of 45°. At normal incidence no anisotropy has been observed, which indicates a homogenous distribution of the transition dipole moment vectors. With a change in the angle of incidence from 0 to 30° or 45 or 60°, change in absorbance for parallel and the perpendicular components is observed. This indicates that the aggregated B(*b*)F molecules have a preferred orientation in the LB films. We have estimated the orientation of the molecules in the film from the relation [35]

$$D = \frac{2 - \tan^2\beta}{\tan^2\beta \dfrac{1 + \cos^2\alpha}{\sin^2\alpha} + 2}$$

where D is the linear dichroism, α is the angle of incidence and β is the angle between the transition dipole moment vector of the molecule and the normal to the plane of the monolayer. In this case, the average value of β for angle of incidences of 30°, 45° and 60°, is found to be 38.6°. The orientation of the molecules derived from linear dichroism study should be taken as the average value over the entire LB film.

5. Emission spectroscopy

In Fig. 3, we have plotted the emission spectra of the LB film of B(*b*)F in SA matrix at different mole fractions (0.1–0.6 M) of B(*b*)F along with the emission spectra in ethanol solution and also of B(*b*)F MC at room temperature for comparison. The emission spectrum of B(*b*)F in ethanol solution (1×10^{-6} M) shows a broad band with an overlapping structure in the 390–550 nm region with the maximum at about 450 nm and is in excellent agreement with the literature [36]. Emission spectrum of mixed LB film of B(*b*)F–SA, for all mole fractions B(*b*)F, are red shifted and a prominent shoulder at about 420 nm was observed in comparison to the solution spectra. This shoulder may arise due to change in relative intensity distribution among various vibrational bands in the fluorescence spectrum of the mixed LB film. The red shifted spectra may be explained in terms of interactions between the B(*b*)F molecules with different orientation or packing in the LB film structures [33]. This seems to indicate that the B(*b*)F molecules in the mixed LB films form low dimensional microcrystalline aggregates. Similar results have also been reported for other nonamphiphilic molecules incorporated in the LB films [7,11].

We have studied the decay characteristics of the emission bands at 420 and 460 nm with excitation at 338 nm. The decay curves are well fitted considering

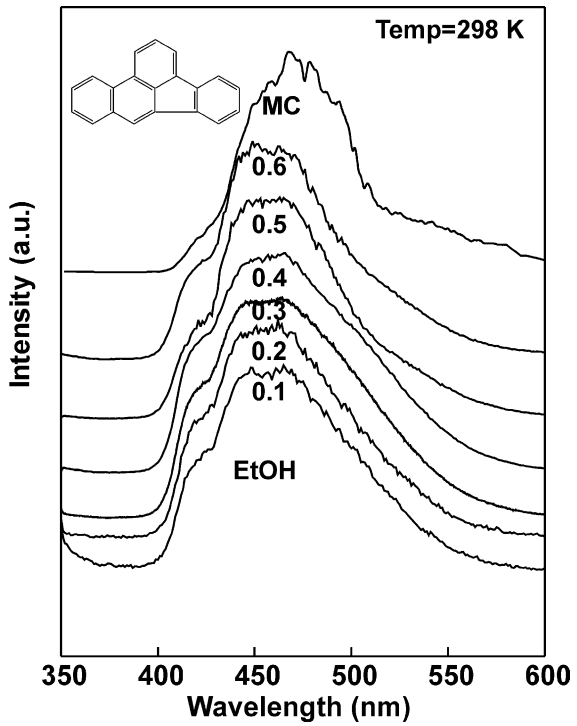

Fig. 3. Emission spectra of B(*b*)F in EtOH, MC and mixed LB films with SA at different B(*b*)F mole fractions. The inset shows the structure of B(*b*)F molecule.

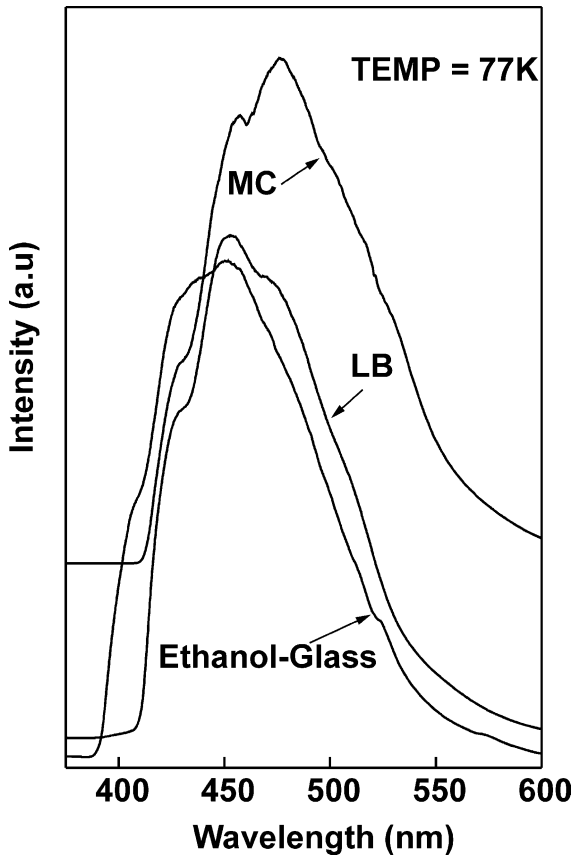

Fig. 4. Emission spectra of B(*b*)F at 77 K in ethanol glass matrix (EtOH–glass), mixed LB film (10 bilayer; 0.5 M of B(*b*)F) and in B(*b*)F MC.

uniexponential curve. On analyzing the decay of the emission at 420 and 460 nm, we found $\tau = 24$ ns ($\chi^2 = 1.02$). This indicates that the bands are of same origin. The fluorescence lifetime of B(*b*)F in ethanol solution (29 ns) was reported by Millican et al. [37] using phase resolved excitation–emission matrix method. As hopping of the excitation energy between neighboring molecules makes energy transfer an efficient process [38,39], in the multilayer LB films this process may occur. This type of energy transfer may be the reason of decrease in lifetime of the B(*b*)F–SA LB film.

Fig. 4 shows the emission spectra of B(*b*)F in dilute ethanol glass (1×10^{-6} M), mixed LB film (0.5 M of B(*b*)F) and B(*b*)F MC with the excitation at 300 nm at low temperature (77 K). The emission spectrum of B(*b*)F in ethanol glass shows no abrupt change in the peak position in comparison to the spectrum at room temperature (298 K) except that a shoulder at ~408 nm is prominent. In the LB film, this shoulder is red shifted to 430 nm and other two emission bands at positions 455 and 472 nm are observed. However, the relative intensity of the band at 430 nm is less in comparison to the low energy band at 455 nm. In comparison with the emission of MC at 77 K, it is found that all these bands exist. The band at 455 nm is quenched and the band at 472 nm increases in intensity and becomes broadened. From the close similarity between the spectra of MC and LB film, it seems that B(*b*)F in the mixed LB film form low dimensional microcrystalline aggregates.

Fig. 5 shows the phosphorescence spectra of B(*b*)F in ethanol glass, in mixed LB film (0.5 mole fraction of B(*b*)F) and B(*b*)F MC at 77 K. The existence of phosphorescence indicates that in the excited state, there is a cross-over from the singlet to triplet state. In ethanol glass matrix, the phosphorescence spectrum shows a structured band system with its 0–0 band at 530 nm. Monitoring at phosphorescence emission maxima gives a phosphorescence lifetime of 119 ms. The phosphorescence spectrum of B(*b*)F–SA mixed LB film is also shown in Fig. 5. In LB film all the bands are broadened. The broadening in the spectrum suggests that in mixed LB film, instead of discrete triplet energy level, a band is formed. This is due to the closer proximity of the B(*b*)F molecules in the mixed LB film unlike that in solution. It is interesting to note that for LB film the high-energy band at 530 nm is considerably quenched whereas the low energy bands at 575 and 640 nm are enhanced, considerably. Similar observation is obtained for the B(*b*)F MC phosphorescence spectrum.

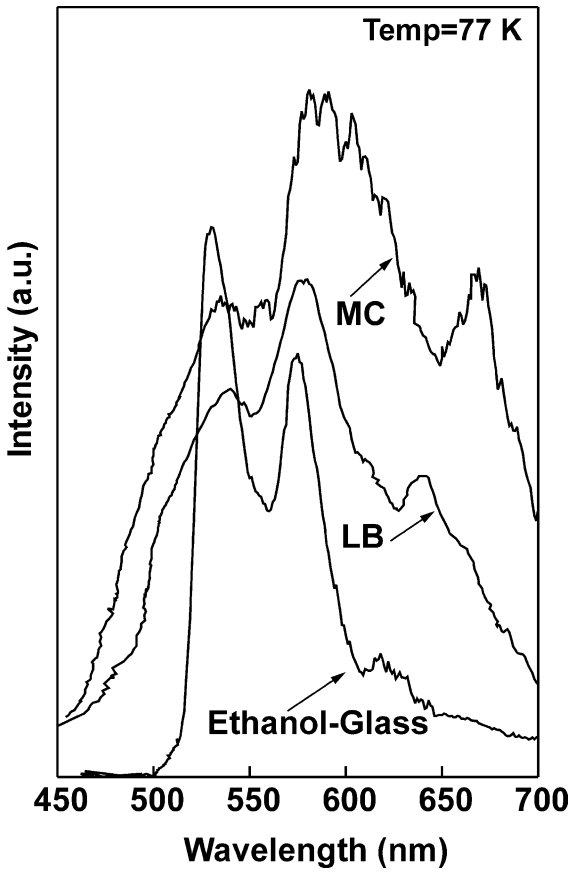

Fig. 5. Phosphorescence spectra of B(*b*)F at 77 K in ethanol glass (EtOH–glass), mixed LB film (10 bilayer; 0.5 M of B(*b*)F) and B(*b*)F MC.

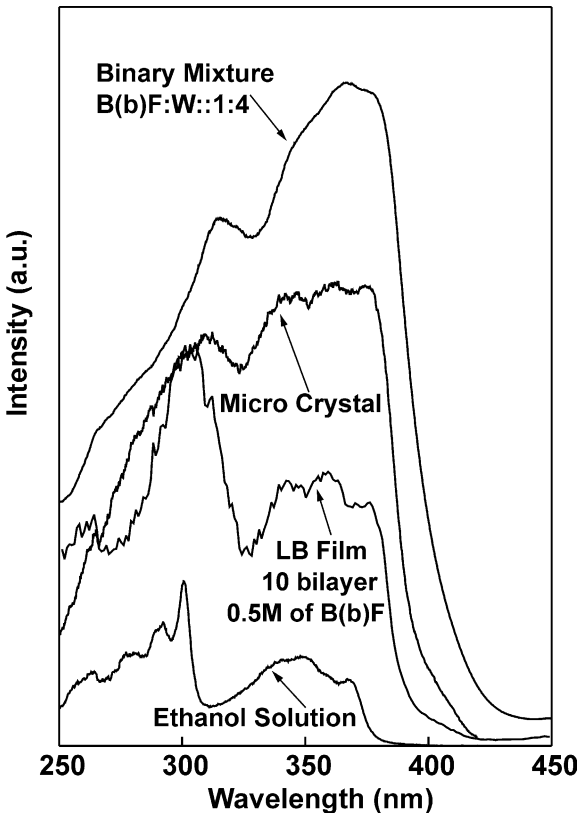

Fig. 6. Plot of excitation intensity of B(*b*)F vs. wavelength at 298 K.

The steady decrease in the intensity of the high-energy phosphorescence band in LB film and MC is probably due to the reabsorption effect. We have measured the phosphorescence lifetime of LB film and B(*b*)F MC, which are 35 and 20 ms, respectively. The considerable shorter phosphorescence lifetime in LB film and MC compared to ethanol glass matrix indicates an efficient deactivation process, which is known to increase in aggregates and crystals. The distinct similarity with the MC suggests the formation of microcrystalline aggregates in the mixed LB film.

6. Excitation spectra

Fig. 6 shows the excitation spectra of B(*b*)F in ethanol solution (1×10^{-6} M), ethanol–water mixture, MC and mixed LB film. The excitation spectrum of B(*b*)F in ethanol solution monitored at its emission maxima gives rise to a structured spectrum and is in good agreement with the absorption spectrum. The 0–0 band of the ethanol–water binary mixture (BIN) is located at 378 nm, which is red shifted by about 8 nm relative to the 0–0 band at 368 nm in pure ethanol solution. The broadening and red shift of the excitation spectra provide evidence of preassociation of the B(*b*)F moieties in the ground state, which is justified in view of the strong hydrophobic nature of the B(*b*)F molecules, which form aggregates. The excitation spectrum of the LB film of B(*b*)F–SA monitored at 420 and 460 nm are found to be identical and a broad band profile in the region of 275–325 nm with the 0–0 band located at 378 nm. Such a broad profile associated with a red shift of the 0–0 band suggests aggregation in the LB film. The excitation spectrum of B(*b*)F MC at room temperature has been recorded for comparison. The spectra of multilayered LB film and the MC are similar, which confirms the formation of microcrystalline domains in the multilayered LB film. The difference in the intensity distribution and the shape of the excitation spectra reflects the interaction between the B(*b*)F molecule and their microenvironment. This confirms the different molecular packing in different microenvironment, which seems to be justified as molecular packing in the crystals, are known to be largely dependent on the method of their preparation [40].

7. Conclusion

Nonamphiphilic B(*b*)F molecules mixed with SA have been incorporated successfully in LB film. The increase of stability of the mixed monolayer in comparison to the pure one indicates the fair compatibility of the guest and host. Repulsive types of interactions between B(*b*)F and SA molecules is indicative of the formation of aggregates. From the polarized absorption spectrum, the average orientation of the B(*b*)F molecules are found to be 38.6° over the LB films. The reabsorption effect is dominant in the phosphorescence emission spectra and extent of reabsorption depends on the microenvironment and aggregate size. Shorter phophorescence lifetime supports the formation of aggregates/microcrystalline domains in the mixed LB films.

Acknowledgements

This research was partially supported by D.S.T., Government of India, Grant No. SP/S2/M-25/97. Authors also thankfully acknowledge Prof. M. Chowdhury and Mr Avijit Mondal of Physical Chemistry Department of the same institute for providing the instruments and helping in fluorescence lifetime measurements.

References

[1] H. Kuhn, Thin Solid Films 99 (1983) 1.
[2] S. Baker, M.C. Petty, G.G. Roberts, M.V. Twigg, Thin Solid Films 99 (1983) 53.
[3] A. Ulman, R.P. Scarnige, Langmuir 8 (1992) 894.
[4] R.M. Weiss, M. McConell, Nature 310 (1984) 47.
[5] A. Angelova, M. Van Der Auweraer, F.C. De Schryver, Langmuir 11 (1995) 3165.
[6] S. Acharya, T.K. Parichha, G.B. Talapatra, Mol. Mater. 12 (2000) 91.
[7] A.G. Vitukhnovsky, M.I. Sluch, J.G. Warren, M.C. Petty, Chem. Phys. Lett. 173 (1990) 425.
[8] S. Acharya, D. Bhattacharjee, G.B. Talapatra, Chem. Phys. Lett. 352 (2002) 429.
[9] S. Acharya, D. Bhattacharjee, G.B. Talapatra, J. Colloid Interface Sci. 244 (2001) 313.
[10] A. Ulman, An Introduction to Ultrathin Organic films: From Langmuir–Blodgett films to Self Assemblies, Academic Press, New York, 1991.
[11] A.K. Dutta, Phys. Chem. 99 (1995) 14758.
[12] A.K. Dutta, T.N. Misra, A.J. Pal, Langmuir 12 (1996) 359.
[13] K. Ray, D. Bhattacharjee, T.N. Misra, J. Chem. Soc. Faraday Trans. 93 (22) (1997) 4041.
[14] S. Yu Arzhantsev, S. Takeuchi, T. Tahara, Chem. Phys. Lett. 330 (2000) 83.
[15] J. Cha, Y. Park, K. Lee, T. Chang, Langmuir 15 (4) (1999) 1383.
[16] P.A. Antunes, C.J.L. Constantino, R.F. Aroca, J. Dufft, Langmuir 17 (10) (2001) 2958.
[17] A.K. Kirsch, A. Schapar, H. Huesmann, M.A. Rampi, D. Möbius, T.M. Jovin, Langmuir 14 (1998) 3895.
[18] P.N. Prasad, D.J. Williams, Nonlinear Optical effects in Molecules and Polymers, Wiley, New York, 1991.
[19] R. Niessner, P. Wilbring, Anal. Chem. 61 (1989) 708.
[20] D.V. O'Connor, D. Phillips, Time-correlated Single Photon Counting, Academic Press, New York, 1965.
[21] S. Basu, D.N. Nath, M. Chowdhury, Chem. Phys. Lett. 161 (1989) 449.
[22] A.K. Dutta, T.N. Misra, A.J. Pal, J. Phys. Chem. 98 (1994) 4365.
[23] A.K. Dutta, T.N. Misra, A.J. Pal, J. Phys. Chem. 98 (1994) 12844.
[24] G.L. Gaines Jr., Insoluable Monolayers at the Liquid–Gas Interface, Interscience, New York, 1966.
[25] A.W. Adamson, Physical Chemistry of Surface, Wiley, New York, 1990.
[26] H. Ito, T.H. Morton, V. Vodyanoy, Thin Solid Films 180 (1989) 180.
[27] T.K. Parichha, G.B. Talapatra, Opt. Mater. 11 (1998) 9.
[28] H.W.D. Stubbs, S.H. Tucker, J. Chem. Soc. (1954) 227.
[29] J. Koutecky, P. Hochman, J. Michl, J. Chem. Phys. 44 (1964) 2439.
[30] E.G. McRae, M.J. Kasha, Chem. Phys. 28 (1958) 721.
[31] M. Kasha, A.R. Rawals, M.R. El-Bayaumi, Pure Appl. Chem. 11 (1965) 37.
[32] H. Bucher, H. Kuhn, Chem. Phys. Lett. 6 (1970) 183.
[33] V. Czikklely, H.D. Forsterling, H. Kuhn, Chem. Phys. Lett. 6 (1970) 207.
[34] R. Weinberger, L. Clinelove, Spectrochim. Acta A 40 (1984) 49.
[35] C.N. N'soukpoe-Kossi, J. Sielewiesiuk, R.L. Leblance, R.A. Bone, J.T. Landrum, Biochim. Biophys. Acta 940 (1985) 255.
[36] A. Sharma, O.S. Wolfbeis, Spectrochim. Acta 43A (1987) 1417.
[37] D.W. Millican, B.L. McGown, Anal. Chem. 61 (1989) 580.
[38] G. Zumofen, A. Blumen, Chem. Phys. Lett. 98 (1984) 393.
[39] A. Blumen, G. Zumofen, J. Lumin, J. Lumin. 24/25 (1981) 781.
[40] A.K. Dutta, J. Phys. Chem. B 101 (1997) 569.